INTERIM REPORT

Accession No. 7909240749

Contractor's Report No. _____

Contract Program or Project Title: HEPA Filter Tests Study

Subject of this Document: Progress reported for April 1-June 30, 1979

Type of Document: Informal progress report

Author(s): Henry L. Horak, W. S. Gregory, and R. A. Martin

Date of Document: August 28, 1979

Responsible NRC Individual and NRC Office or Division: _____

Donald E. Solberg, Systems Performance Research Branch, SAFER:RES

This document was prepared primarily for preliminary or internal use. It has
not received full review and approval. Since there may be substantive changes,
this document should not be considered final.

LOS ALAMOS SCIENTIFIC LABORATORY
UNIVERSITY OF CALIFORNIA
P.O. BOX 1663
LOS ALAMOS, NEW MEXICO 87545

DISTRIBUTION:
S. Levine, RES
C. Beck, RES
J. Ayer, NMSS
A. Clark, NMSS
M. Au, NMSS
P. Loysen, NMSS
G. Kligfield, NMSS
L. Rouse, NMSS
M. Weinstein, SD

Prepared for
U.S. Nuclear Regulatory Commission
Washington, D.C. 20555

NRC FIN No. A7028

NRC Research and Technical
Assistance Report

INTERIM REPORT

999 345

University of California

LOS ALAMOS SCIENTIFIC LABORATORY

Post Office Box 1663 Los Alamos, New Mexico 87545

in reply refer to: WX-8-3037 (R295)
Mail stop: 928

August 28, 1979

Mr. Donald E. Solberg
Systems Performance Branch
Division of Safeguards
Fuel Cycle and Environmental Research
US Nuclear Regulatory Commission
Washington, DC 20555

Dear Don:

SUBJECT: R295 QUARTERLY PROGRESS LETTER (APRIL 1 - JUNE 30, 1979)

This quarter our investigations have included the following three areas:

A. pretesting analysis of fans,

B. full-scale configuration of the laser Doppler particle counter, and

C. standard testing of filter medium samples taken from tornado-tested filters.

This letter summarizes our results in each of these work areas. Detailed information for each area is included in the appendices.

I. RESULTS

A. Pretesting Analysis of Fans

Until now we have tested only High Efficiency Particulate Air (HEPA) filters. The next ventilation system components we will study under simulated tornado transient conditions are fans. A simple similitude study of fans was performed to aid in selection of the appropriate fan models for testing and to provide guidelines for designing our experiments and interpreting the results. We are now ready to specify and procure the fans needed for testing in this program. Details may be found in Appendix A.

B. Full-Scale Configuration of the Laser Doppler Particle Counter

Modifications to the laser Doppler particle counter are explained in Appendix B. The data signal-to-noise ratio is better than reported earlier. The configuration is shown in Fig. 1.
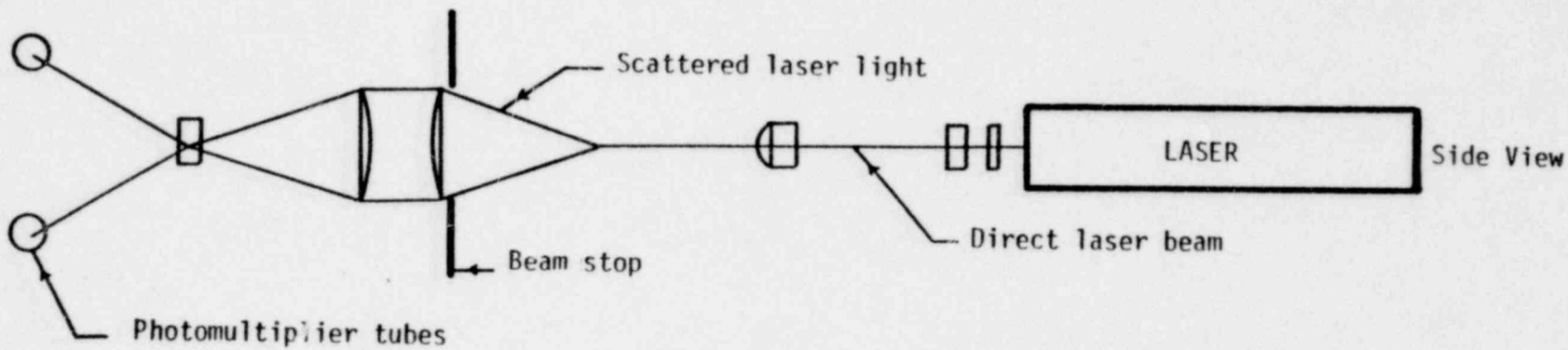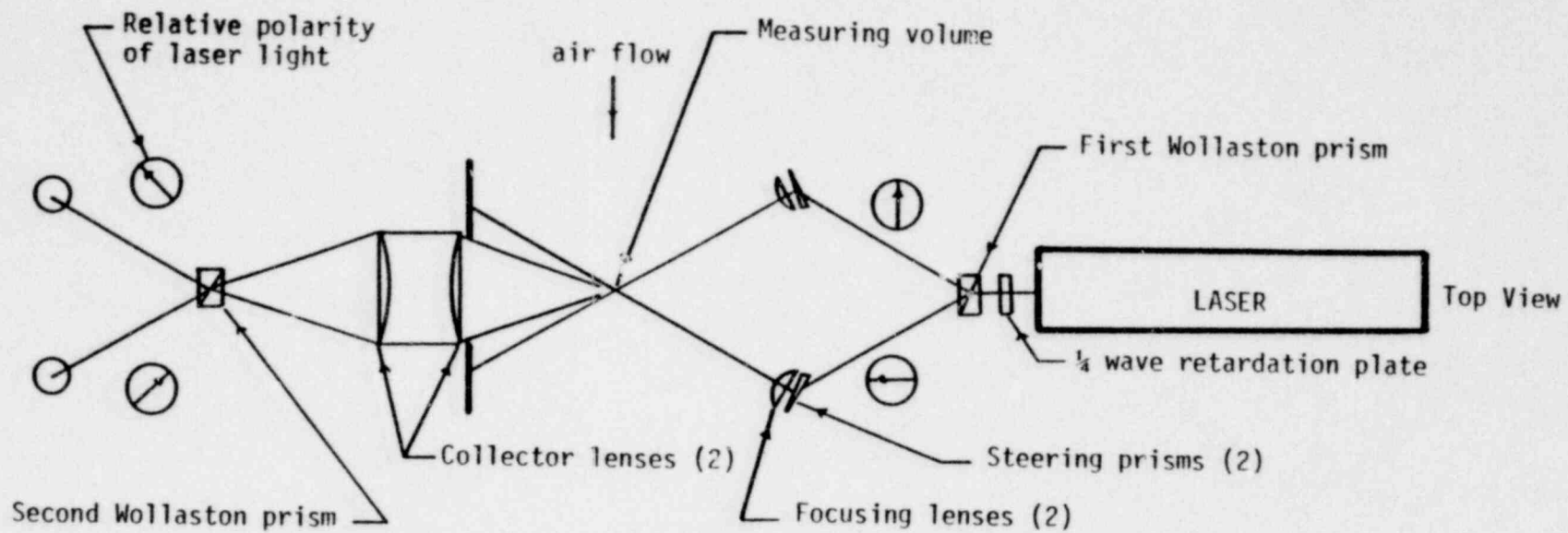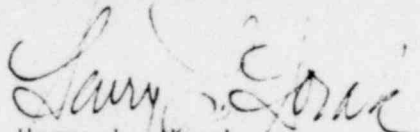
999 346

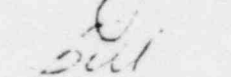Fig. 1. LDV particle counter schematic.

C. Standard Testing of Filter Medium Samples Taken from Tornado-Tested Filters

We took filter medium samples from 12 previously tornado-tested HEPA filters and performed strength tests on them at the Rocky Flats HEPA Filter Acceptance Laboratory. The methodology and test procedure are explained in Appendix C. The quantitative results have not been analyzed yet. However, preliminary analysis indicates a correlation between the weakest filters and media that did not meet Department of Energy (DOE) specifications when tested after the tornado simulation.

II. SUMMARY

We have performed the pretesting fan analysis and are ready to size the test fans. The laser Doppler particle counter is being tested in its final configuration. We strength-tested the media from 12 HEPA filters previously tested on our tornado simulator.

Henry L. Horak

W. S. Gregory

R. A. Martin

HLH/WSG/RAM:kmt

Cys: M. L. Brooks/L. W. Hantel, WX-DO, MS 686
       W. G. Davey, Q-DO, MS 561
       W. A. Bradley, WX-8, MS 928
       H. A. Lindberg, WX-8, MS 928
       ISD-5 (2), MS 150
       File

APPENDIX A

FAN PRETESTING ANALYSIS

I. FAN TESTING - BACKGROUND

Flow behavior in filters, dampers, system volumes, and fans must be understood to predict overall ventilation system performance. The fans will be the first components to be affected by a tornado depressurization at the exhaust stack. To calculate the filter pressure drop and flow rate using TVENT[1], we need fan performance data for steady-state and transient conditions for both normal and off-design behavior. Unfortunately, little information is available on fan performance outside the normal operating region for steady flow.

Accordingly, we have initiated a fan testing program that will generate the necessary normal and off-design data. This program involves testing the two types of fans commonly found in nuclear facility ventilation systems, centrifugal and vaneaxial. For high heads, up to 15 in. w.g. (103 kPa), centrifugal fans are best suited for moving moderate volumes of air. For lower heads, up to 5 in. w.g. (35 kPa), vaneaxial fans are useful if relatively large flows are needed.

Our testing objective is to experimentally evaluate the performance of both types of fans under simulated tornado pressure transients. We anticipate that tornado transients may induce backflow or outrunning flow in the fan. Backflow occurs when the flow direction in the fan is forced to reverse itself so that the flow rate becomes negative at high pressure heads. Outrunning flow occurs when more air flows through the fan than it could normally deliver at zero fan static pressure. For outrunning flow, the fan static pressure becomes negative at high flow rates.

We will simulate tornado pressure transients using our existing blowdown facility located at the New Mexico State University at Las Cruces. This is the same experimental facility that has been used for HEPA filter structural testing.

Each fan manufacturer offers the ventilation system design engineer a wide selection of sizes and speeds in a particular fan model line. The design engineer can then trade off cost with performance characteristics to arrive at an economical selection. To test all of the available fan models is impractical. Furthermore, we are limited by our blowdown facilities to flows of about 25 000 cfm (11.8 m^3/s), so we cannot realistically simulate a tornado pulse through a fan designed for flows larger than this figure.

As a result, we have turned to dimensional analysis and dynamic similitude[2] to select representative fans that are within the capacity of the test facility. The use of dimensionless parameters is highly desirable because they permit limited experimental results to be applied to different fan sizes, rotational speeds, and flow densities. Further, they permit a generalization of the experimental data so that the phenomenon is described in its entirety and not restricted to a single specialized experiment. Use of dimensionless parameters also allows the data to be presented in a more compact and meaningful way. Finally, the use of similitude will allow us to perform the least number of tests of the fewest number of fans of the smallest size, thereby saving time and money.

999   3

II. FAN SIMILITUDE THEORY

A. General

Fan similitude theory is not difficult. In fact, the dimensionless ratios (scaling laws) for fans have been known for many years and used extensively by the fan manufacturers in their testing programs. However, the question arises as to whether the similitude relations hold under transient conditions. We think that they do, but this can and should be verified by experiment.

We will briefly review the similitude analysis to illustrate the technique, to bring out the assumptions involved, and to summarize the results. Our goal in this exercise is to select only two fans of each type (centrifugal and vaneaxial) of a size compatible with our facility limitations, and from experimental tests of these, predict the performance of any fan from the same series under both ste~' ind transient flow conditions. By testing two fans of each type, we will be able to check the similitude laws we develop.

The value of this analysis resides in the fact that if we can create the same geometric and force ratios in a model fan experiment as occur on the full-scale fan, then the dimensionless solution for the model is valid also for the prototype.

B. Centrifugal Fans

We begin by identifying all of the pertinent variables that affect the air moving process of the fan. These seven variables are

Q = volume flow rate cfm (m^3/s),

N = blower rotational speed rpm,   (A-1a)

D = fan size characteristic (rotor diameter), ft (m),

ρ = fluid density, lbm/ft^3 (kg/m^3),

Δp = pressure rise (head) produced by fan, in. w.g. (Pa), (A-1a)

μ = fluid viscosity, lbm/ft s (Pa s), and

e = fluid bulk modulus of elasticity, lbf/in.^{2} (Pa).

The dimensions involved in these quantities are

$Q \sim L^3 T^{-1}$,

$N \sim T^{-1}$,

$D \sim L$,

$\rho \sim ML^{-3}$, (A-1b)

$\Delta p \sim ML^{-1}T^{-2}$,

$\mu \sim M^{-1}T^{-1}$, and

$e \sim ML^{-1}T^{-2}$.

We note that in selecting the variables listed in Eq. (A-1), we have neglected effects caused by surface tension and gravitational forces (as reflected in the Weber number and Froude number). We also assume that the fluid properties ρ, μ, and e are constant (small fluid temperature changes).

As three dimensions are involved in Eq. (A-1b), namely, M, L, and T, the Buckingham π-theorem tells us that the quantities in Eq.(A-1) may be arranged into 7-3 = 4 independent dimensionless parameters. Once we know these parameters, then similitude theory tells us that a true model of a given physical system must be designed and operated so that every π group of the model should be equal in magnitude to the corresponding π group of the prototype (full size) system. Thus, it is the π groups that determine how the model is designed and how the experimental results are scaled once obtained.

We can now write the functional relationship

$F(Q, N, D, \rho, \Delta p, \mu, e) = 0$. (A-2)

Choosing D, N, and ρ as the repeating variables, we find the following four π
groups:

$$\pi_1 = \frac{\Delta p}{D^2 N^2 \rho} \quad ,$$

$$\pi_2 = \frac{Q}{D^3 N} \quad ,$$

$$\pi_3 = \frac{\mu}{D^2 N \rho} \quad , \quad \text{and} \tag{A-3}$$

$$\pi_4 = \frac{e}{D^2 N^2 \rho} \quad .$$

Thus we have established a new functional relationship,

$$F_1\left(\frac{\Delta P}{D^2 N^2 \rho}, \ \frac{Q}{D^3 N}, \ \frac{\mu}{D^2 N \rho}, \ \frac{e}{D^2 N^2 \rho} \right) = 0 \quad . \tag{A-4}$$

Because they are dimensionless, any one of the π groups may be inverted or
raised to any other power. For convenience we invert π_3 and π_4 and take
the square root of π_4 to get

$$F_2\left(\frac{\Delta P}{D^2 N^2 \rho}, \ \frac{Q}{D^3 N}, \ \frac{\rho N D^2}{\mu}, \ \frac{N D}{\sqrt{(e/\rho)}} \right) = F_2(\pi_1, \pi_2, \pi_3, \pi_4) = 0 \quad . \tag{A-5}$$

Henceforth, our π groups will be the expressions in parentheses in
Eq. (A-5). The first two groups, π_1 and π_2, characterize homologous fans
provided the fans are geometrically similar. For dynamic similitude to hold

between model and prototype, we equate π groups. As we equate terms, we use
the relations

$$\rho_p = \rho_m \, ,$$

$$\mu_p = \mu_m \, , \text{ and} \qquad\qquad (A-6)$$

$$e_p = e_m ,$$

because the only practical set-up for us is to use air in both prototype (p)
and model (m). (Note that this is a practical, not a theoretical limitation.)

$$\pi_1 : \left(\frac{\Delta P}{D^2 N^2}\right)_P = \left(\frac{\Delta P}{D^2 N^2}\right)_m$$

$$\frac{\Delta P_p}{\Delta P_m} = \left(\frac{D_p}{D_m}\right)^2 \left(\frac{N_p}{N_m}\right)^2 \qquad\qquad (A-7)$$

$$\pi_2 : \left(\frac{Q}{D^3 N}\right)_P = \left(\frac{Q}{D^3 N}\right)_m$$

$$\qquad\qquad (A-8)$$

$$\frac{Q_p}{Q_m} = \left(\frac{D_p}{D_m}\right)^3 \left(\frac{N_p}{N_m}\right)$$

$$\pi_3 : \quad (ND^2)_p = (ND^2)_m \quad \text{(not satisfied)} \qquad\qquad (A-9)$$

$$\pi_4 : \quad (ND)_p = (ND)_m \qquad\qquad (A-10)$$

Clearly, the requirements $\pi_{3P} = \pi_{3m}$ in Eq. (A-9) and $\pi_{4P} = \pi_{4m}$ in
Eq. (A-10) are contradictory.

Let us look more closely at the meaning of the π terms in Eq. (A-5).
Identify the fan blade tip speed as $V_t = ND$. Then $\pi_1 = \Delta P / \rho V_t^2$ is the

pressure coefficient based on the tip speed. Next, because the flow area is proportional to the square of the blade diameter,

$$\pi_2 = \frac{Q}{D^3 N} = \frac{Q/A}{ND} = \frac{V_f}{ND} = \frac{V_f}{V_t} \quad .$$

This says that the fans must have the same ratio of fluid velocity (V_f) to peripheral speed. Then,

$$\pi_3 = \frac{\rho ND^2}{\mu} = \frac{\rho V_t D}{\mu} \quad ,$$

which is the familiar Reynolds number or ratio of inertia forces to viscous forces based on the blade tip speed. Finally,

$$\pi_4 = \frac{ND}{\sqrt{e/\rho}} = \frac{V_t}{a} \quad ,$$

where a is the acoustic velocity in the fluid. Thus, π_4 is the familiar Mach number (square root of Cauchy number) or ratio of the inertia forces to the compressibility (or elastic) forces. Therefore, if we impose $\pi_{4p} = \pi_{4m}$, then we are matching force ratios that compare compressibility effects. Equation (A-10) tells us that to do this we should run our fans at the same tip speed. The viscous forces appearing in π_3 and the compressibility forces in π_4 are of less importance than the pressure forces in π_1.

Apparently, for Eq. (A-6) to hold, we cannot match both the viscous effects, Eq. (A-9), and the compressibility affects, Eq. (A-10). One of these π groups must be violated or distorted. This is a well-known and understood problem in fluid modeling. In our case, we choose to distort π_3, the Reynolds number or viscous effects because in the models we will be testing, the Reynolds number will be very high (turbulent flow).

999   35

Consequently, the relative changes in Reynolds number caused by viscosity distortion should be small, and the resulting modeling errors should be small (2 or 3 %). In distorting π_3 we are anticipating the local mach number variations (in the flow over the rotating blades) to be more important to fan performance than the local Reynolds number variations.

Returning to Eqs. (A-7) through (A-10), if we use Eq. (A-10), Eq. (A-7) becomes

$$\frac{\Delta P_p}{\Delta P_m} = 1 \qquad \text{or} \qquad n_p = 1 \ . \tag{A-11}$$

Eq. (A-8) becomes

$$\frac{Q_p}{Q_m} = \left(\frac{D_p}{D_m}\right)^2 \qquad \text{or} \qquad n_Q = n_D^2 \ , \tag{A-12}$$

and Eq. (A-10) may be rewritten

$$\frac{N_p}{N_m} = \frac{D_m}{D_p} \qquad \text{or} \qquad n_N = \frac{1}{n_D} \ . \tag{A-13}$$

Because $A \sim D^2$, Eq. (A-12) may be rewritten

$$\frac{Q_p}{A_p} = \frac{Q_m}{A_m} \ ,$$

so $V_{fp} = V_{fm}$ \qquad or \qquad $n_{vf} = 1$. \hfill (A-14)

Because $V_f \sim D/t$,

$$V_{fp}/V_{fm} = \frac{D_p/t_p}{D_m/t_m} = 1 \ ;$$

999   350

then

$$\frac{D_p}{D_m} = \frac{t_p}{t_m} \qquad \text{or} \qquad n_t = n_D \ . \qquad\qquad \text{(A-15)}$$

In Eqs. (A-11) through (A-15), we have defined the pressure scale $n_p = \Delta P_p/\Delta P_m$, the flow rate scale $n_Q = Q_p/Q_m$, the length scale $n_D = D_p/D_m > 1$, the rotational speed scale $n_N = N_p/N_m$, the velocity scale $n_V = V_{fp}/V_{fm}$ and the time scale $n_t = t_p/t_m$.

To summarize, we see from π_1 and π_2 that for similitude to hold (approximately), we must choose our fan pairs from a homologous series. Being unable to match both π_3's and π_4's (for practical reasons), we elect to match π_4's (compressibility) for the most accurate model. The π_4's will be matched if we run our prototype and model at the same tip speed. Finally, Eqs. (A-11) through (A-15) tell us how to design our experiments and interpret the results.

C. Axial Fans

Because vaneaxial fans have symmetrical centerbodies called hubs behind which the motors are mounted, there is one additional pertinent variable, a second length of importance besides the blade tip diameter, D. This second variable is the hub diameter, H. The similitude analysis follows that for centrifugal fans above except that the addition of another variable means there will be one more (or 8-3 = 5) π group. The new group is simply $\pi_5 =$ H/D or the hub to tip ratio or simply "hub ratio." Thus, in addition to the π

groups discussed above, for vaneaxial fans we impose $\pi_{5p} = \pi_{5m}$.

Otherwise, the results from Section B apply here.

In the coming quarter we will be specifying and procuring both centrifugal

and axial fans for testing in this program.

REFERENCES

1. K. H. Duerre, R. W. Andrae, and W. S. Gregory, "TVENT - A Computer Program for Analysis of Tornado-Induced Transients in Ventilation Systems," Los Alamos Scientific Laboratory report LA-7397-M (July 1978).

2. V. L. Streeter and E. B. Wylie, Fluid Mechanics (McGraw-Hill Book Company, Inc., New York, 1975).

APPENDIX B

OPTICAL REMOVAL OF SIGNAL PEDESTAL

The advantages to be obtained by optical removal of the Doppler signal pedestals include better signal-to-noise ratios and improved Doppler data when particle velocities vary greatly in a small time frame. The use of orthogonally polarized light for the two beams seems to be the most preferred method according to the literature reviewed.

By placing a quarter-wave retardation plate at the laser output set at 45° from the fast axis, circularly polarized light is obtained. This is then split by use of a Wollaston prism into two orthogonally polarized beams. Rotation of the first Wollaston prism determines the plane of the two polarized beams. As shown in the drawing, the two beams are in the horizontal plane. The beam divergence angle is determined by the Wollaston prism; this is approximately 20° for the two Wollastons used in this setup. The distance from the first Wollaston determines the beam separation, and by use of the steering prisms and the focusing lenses, the angle of intersection of the two beams at the cross-sectional volume is determined. The angle is approximately 26° in this setup. Care is taken to have each lens focus at the beam intersection.

The intersecting beams are masked off, and the collector lens system images scattered light at the cross-section area on the second Wollaston prism. The latter is oriented at 45° to the plane of the intersecting beams. The scattered light passing through the second Wollaston prism is separated into the $+45^\circ$ and -45° polarized components and is received by the two photomultiplier tubes. A polarizer of the corresponding polarization components is also placed in front of the phototubes.

The signals received at each photomultiplier tube should be equal and 180° out of phase. Thus, subtraction of one signal from the other cancels out the pedestal, whereas the higher frequency Dopper signals are reinforced.

The system has been assembled and is now in operation. Preliminary results are good. Signal-to-noise ratio has been greatly improved. However, we are still experiencing a photomultiplier signal balancing problem. This problem can be solved, but it is a time-consuming task.

APPENDIX C

STANDARD HEPA MEDIUM QUALITY ASSURANCE TESTS

HEPA filters often fail during the tornado simulations when the downstream medium folds tear out. Therefore, we wanted to determine the filter medium strength to find possible correlations with failure pressure under tornado conditions.

The DOE Filter Acceptance Laboratory at Rocky Flats Laboratory has the test equipment to determine medium strength. DOE does not require representative medium testing for HEPA filters, just overall filter resistance and dioctyl phthalate (DOP) penetration testing. However, the acceptable strength and DOP penetration of media have been defined by DOE[*]. These values follow.

1. Minimum tensile strength parallel to the machine direction[**] is to be 2.5 lbs per in. width,

2. minimum tensile strength perpendicular to the machine direction is to be 2.5 lbs per in. width,

3. minimum tensile strength across a medium fold is to be 1.25 lbs per in. width,

4. resistance to air flow at 5.3 cm/s is to be less than 40 mm of water,

5. DOP penetration is to be 0.03% at a flow rate of 5.3 cm/s, and

6. medium thickness is to be greater than 1.5×10^{-2} in. and less than 4×10^{-2} in.

Because Rocky Flats has the equipment and expertise to perform the tests, we sent the medium samples there for testing. We chose three representative

---

[*]MIL-F-51079A, March 31, 1970.

[**]Machine direction is parallel to the direction of medium motion as it passes through the paper machine.

filters from each manufacturer and took eight samples from each. Four samples

per filter came from the flat internal part of the medium; four came from the

folded part of the medium. For each filter, the samples were taken at both

edges, and at distances of one-third and two-thirds across the filter face.

These filters had already failed in our tornado simulator, but the samples

were not visibly damaged. We will report the test results and subsequent

analyses in the next quarter.

999   362